Research on Engineering Structures & Materials
www.jresm.org
Research Group

Research Article

Effect of GGBFS and fly ash proportions on fresh, tensile and cracking features of alkali activated concrete with low NaOH concentrations

Mangalapuri Venkateswarlu*[a], T.D Gunneswara Rao[b]

Department of Civil Engineering, National Institute of Technology, Warangal, India

Article Info

Article history:

Received 02 Nov 2023
Accepted 12 Mar 2024

Keywords:

Fly Ash;
GGBFS;
Alkali activated concrete;
Tensile stress;
Tension stiffening sffect;
Cracking characteristics

Abstract

This study mainly investigated the tensile and cracking features of ash alkali activated concrete with different slag-fly ash proportions and low NaOH concentrations cured at ambient temperature. High-molarity NaOH leads to risk and is costly, whereas, in field conditions, heat curing is difficult. Therefore, in this study three mixes (mix-A, B and C) were developed using 0/100, 20/80, 40/60, 60/40, 80/20, and 100/0 slag-fly ash proportions in this study. Sodium hydroxide (SH) and sodium silicate (SS) were used as activators and concentrations of sodium hydroxide were used as 1M, 2M and 4M in mixes A, B and C respectively, but alkaline ratio (SS/SH) was fixed as 1.5 in all the mixes. Slump, and strength aspects (compressive, split tensile, and flexural) were evaluated. The tensile (tensile strength, tension stiffening) and cracking characteristics (crack spacing, crack width) were evaluated under uniaxial tensile loading on reinforced prismatic members. From test outcomes, workability in terms of slump of the composites decreased with increased percentage of slag or granulated blast furnace slag (GGBFS) in the total binder, but the tensile (tensile stress and tension stiffening effect) and compressive strengths increased with increasing percentage of GGBFS. Better cracking properties (i.e., minimum crack widths and reduced crack spacings) were observed when the mixes contained higher percentages of GGBFS. The obtained crack spacings were correlated with CEB-FIP model code, and existing research studies. The crack spacings obtained in this study are consistent with CEB-FIP model code. Finally, this study demonstrated that when slag-fly ash alkali activated concretes were prepared with solutions containing low NaOH concentrations and cured at room temperature (ambient), there was an increase in the strength and cracking properties with higher percentages GGBFS.

1. Introduction

Sustainability and environmental issues are currently the need-of-the-hour in every aspect of development. In this context, utilization of industrial byproducts like fly ash, GGBFS, rice husk ash, Meta kaolinite, etc., play an important role in geopolymer concrete (GPC) and alkali activated concretes (AAC). GGBFS exhibits pozzolanic behaviour and good binding properties in base media with low heat of hydration, and it gives better mechanical and excellent durability characteristics [1]. But there were setting time and workability problems with this slag-based alkali activated concrete (SAAC) [2,3]. However, SAAC is a high brittle material due to the higher volume of GGBFS. This leads to development of shrinkage cracks and microcracks. The inclusion of low-calcium fly ash as a binder result in less strength under ambient curing conditions [4]. Curing condition plays very

*Corresponding author: mv718113@student.nitw.ac.in
[a] orcid.org/0009-0008-7305-6845; [b] orcid.org/0000-0002-9145-044X
DOI: http://dx.doi.org/10.17515/resm2024.67me1102rs

prominent role in development of hydration and strength properties in fly ash-GGBFS alkali activated concretes [5]. Using low concentrations of NaOH instead of high levels of sodium hydroxide for concrete production can reduce the risk and cost associated with it. The NaOH solution molarity plays the prominent role in dissolution of compounds present in source materials such as alumina and silica [5,6]. Alkaline ratio (AR) plays an important role in strength development. High alkaline ratios lead to an uneconomical mix, and a low alkaline ratio leads to poor mechanical strength [6-8]. In the context of sustainability and environmental issues, industrial byproduct like fly ash, and GGBFS play an important role in the preparation of alkali activated geopolymer concrete [9]. As the increase of GGBFS and NaOH concentration, the workability of alkali activated concrete (AAC) decreases and setting times of AAC increased [3, 10-12]. The strength properties of alkali-activated fly ash-slag concretes (AAFSC) increase effectively with increasing slag (GGBFS) and sodium hydroxide molar concentrations, as well as decreasing the solution to binder ratio [10-12].

Knowledge of the tensile behaviour of reinforced concrete (RC) is required for a thorough knowledge of a structure's behaviour under normal and severe situations. In predicting the tensile behaviour of RC prisms, the tension stiffening effect has been extensively utilised [13-18]. All tension at a cracked part of a RC member is sustained by reinforcement. Bond action, however, effectively stiffens the member response and lowers deflections by allowing the concrete to continue to transmit tensile loads between the cracks. This phenomenon, referred to as "tension stiffening," and is essentially to account for the presence of average tensile stresses over zero in cracked concrete [19]. Gribniak et al. [20] developed a stochastic technique for tension stiffening assessment. The behaviour of components made of reinforced concrete under flexure does not necessarily match the tension-stiffening relationship shown in the uniaxial tension test [21-23]. Tension stiffening is crucial for controlling beam deflection [24]. It can be used to estimate multiple crack spacings and crack widths [21,24]. The tensile stress of concrete is reduced marginally by raising the reinforcement ratio. Transverse tensile cracking formed under higher steel stress in specimens having large cross sections [25]. Abdulrahman et al. found that geopolymer concrete has comparable tension-stiffening member behaviour as OPC concrete [26]. Cracks have a prominent effect on serviceability, good looking, and load transfer. A concrete member can easily crack due to its low tensile strength. The experiments gave a wide variety of data utilised to assess cracking characteristics in order to construct empirical equations used in the CEB-FIP Model Code, Eurocode-2, and Marti et al. [17,27,28]. Cracking aspects of reinforced concrete affected by the tension stiffening behaviour between the cracks. The increased tensile stiffness also helps reduce the crack width [29,30]. Tension stiffening significantly affected by the shrinkage [30]. But shrinkage did not influence the measured crack widths when crack spacing and strain between steel and concrete are related [30,31]. Compared to OPC concrete, geopolymer concrete exhibited higher first cracking loads and had less effect on the shrinkage of geopolymer concrete and also shrinkage effects do not need to be considered in GPC [32]. Even though several investigations were carried out on research on alkali-activated binders, in most studies, high molarity NaOH concentrations and heat curing conditions were preferred to study the structural behaviour of the concrete member. But high-molarity NaOH leads to risk and is costly, whereas in field conditions, heat curing is difficult.

2. Research Significance

From the existing literature, it is evident that most of the research studies are focused on fresh, mechanical, and durability characteristics GPC and AAC. Even though many studies have also reported on tensile and cracking characteristics of conventional concrete (OPC) but very few investigations are available on tensile and cracking characteristics of alkali activated and/ or geopolymer concretes. Even though several investigations were carried

out on research on alkali-activated binders, in most studies, high molarity NaOH concentrations and heat curing conditions were preferred to study the structural behaviour of the concrete member. But using a solution with such a high NaOH concentration and high alkaline ratio is risky as well as costly. To overcome these problems, there is a need to develop alkali activated concretes that can be cured in the field using low molarity solutions. Hence, this study mainly emphasizes the tensile (strength) and cracking characteristics of FSAAC with different replacement levels of GGBFS-fly ash, prepared with low concentrations of NaOH in an alkaline solution under ambient curing conditions.

3. Experimental Investigation

3.1. Materials

In this investigation GGBFS and fly ash were used as binders. JSW Cement, Warangal provided the GGBFS, and a Ramagundam thermal power station in Telangana provided the class-F fly ash. The quantity and type of GGBFS were confirmed in accordance with IS 12089-1987 [33], while the fly ash was confirmed with IS 3812-1981 [34]. Fine and coarse aggregates were used in this study and confirmed with IS 383-1970 [35]. Physical characteristics of GGBFS, fly ash, fine aggregate, and coarse aggregate are mentioned in Table 1, whereas the chemical composition of GGBFS and fly ash is reported in Table 1. The ideal fine-to-coarse aggregate proportion for mixes B and C has been chosen as 45%:55% of overall aggregate volume and 30%:70% for mix A. Conplast SP430 superplasticizer (SP) (Fosroc Chemicals) was employed in this study, and this SP conformed with IS 9103-1999 [36] and dosage of SP used reported in Table 3. The alkali activator was a mixture of sodium hydroxide (NaOH) and sodium silicate (Na_2SiO_3) solutions. In mixes A, B, and C, sodium hydroxide pellet concentrations of 1M, 2M, and 4M were employed, respectively. A constant Alkaline Ratio of 1.5 was adopted in wholly mixtures, as determined in earlier investigations [2,6,37].

Table 1. Physical and chemical features of GGBFS, fly ash, and aggregates

Physical and Chemical features	GGBFS	Fly ash	Fine aggregate	Coarse aggregate
CaO (%)	34.21	1.82	-	-
$SiO_2 + Al_2O_3$ (%)	53.86	88.85	-	-
Fe_2O_3 (%)	0.80	4.22	-	-
SO_3 (%)	0.90	0.37	-	-
MgO (%)	7.77	1.03	-	-
Other (Na_2O + LOI) (%)	0.51	1.07	-	-
Density (kg/m^3)	1300	1200	1650	1700
Specific gravity	2.90	2.11	2.63	2.73
Specific surface area (m^2/kg)	355	450	-	-

3.1. Materials

The current study took three mixtures into account, they are known as Mix A, B, and C. Mix-A, Mix-B and Mix-C have been developed using 0/100, 20/80, 40/60, 60/40, 80/20, and 100/0 slag-fly ash proportions as binders. The reason for using three different mixes, different fly ash and GGBFS, and three different molarity NaOH solutions is to achieve at least three standard grades of concrete (20 MPa, 40 MPa, and 60 MPa). Similarly, different proportions of fly ash and GGBFS are used to evaluate strength and cracking properties.

These mix compositions are easier for designers in concrete mix design when low-molarity NaOH solutions are added. The blending and proportioning were done in two phases. In the first phase, each mixture (A, B, and C) was incorporated with 0/100% GGBFS-fly ash proportion. In second phase, in all mixes (A, B, and C), GGBFS was replaced in place of fly ash at an interval of 20%, 40%, 60%, 80%, and 100%. There was an overall total of eighteen mixtures made. For this mix proportioning, the unit weight of AAC was taken as 2400 kg/m3. The mixture proportioning was calculated using that unit weight, which was derived from earlier research [2,37]. The mixing process of AAC is the same as conventional concrete [11,12]. Mix proportioning particulars are reported in Table 2. Following blending, mixes were employed to test the workability. After being removed from the moulds, the specimens were kept to remain at room temperature for curing.

Table 2. Mix proportioning details

Mix	Binder (B)		Alkaline solution (S)		Aggregates		SP (%)	Molarity (M)	S/B ratio
	GGBFS (kg)	Fly ash (kg)	NaOH solution (kg)	Na_2SiO_3 solution (kg)	Fine aggregate (kg)	Coarse aggregate (kg)			
A	-	300	66	99	581	1354	6	1	0.55
	60	240	66	99	581	1354	6	1	0.55
	120	180	66	99	581	1354	6	1	0.55
	180	120	66	99	581	1354	6	1	0.55
	240	60	66	99	581	1354	6	1	0.55
	300	-	66	99	581	1354	6	1	0.55
B	-	400	72	108	819	1001	6	2	0.45
	80	320	72	108	819	1001	6	2	0.45
	160	240	72	108	819	1001	6	2	0.45
	240	160	72	108	819	1001	6	2	0.45
	320	80	72	108	819	1001	6	2	0.45
	400	-	72	108	819	1001	6	2	0.45
C	-	400	80	120	810	990	6	4	0.50
	80	320	80	120	810	990	6	4	0.50
	160	240	80	120	810	990	6	4	0.50
	240	160	80	120	810	990	6	4	0.50
	320	80	80	120	810	990	6	4	0.50
	400	-	80	120	810	990	6	4	0.50

3.4 Tests Performed

To measure the workability of freshly mixed concrete, a slump test was conducted. This slump test was performed as per the Indian standard IS: 7320 [38]. The compressive strengths of concrete cubes (100 x 100 x100 mm) were evaluated using the Tinius-Olsen Testing Machine (TOTM) at 7 and 28 days of curing as per the Indian standard: 516–1959 [39], and its capacity is 2000 kN. For the split tensile strength, a test on a cylinder (100 mm dia. And 200 mm height) was also performed on the same equipment. A three-point loading test on prisms (500 x100 x 100 mm) was done for flexural strength according to ASTM C 293-02 [40]. Corresponding test diagrams were presented in Fig.1(a). Reinforced concrete prismatic specimens of size 600 x 60 x 60 mm were used in this study to explore the tensile and fracture properties. The specimens were subjected to uniform tension loading in a UTM with a capacity of 200 kN. Two linear variable differential transducers (LVDT) were mounted on opposite faces of the concrete prism. The entire test setup is shown in Figs.1(b) and 1(c). The change in axial length (deformation) was measured using these LVDTs. The signals received by the LVDTs were recorded using a DAQ device. Cracks and their formations were observed during the test, and crack spacing was measured for every

1 kN increment of load. The test was continued until the steel bar yielded. During the test, crack widths were observed and measured at every 10 kN load. Maximum crack width values were measured on all surfaces. To establish realistic bar response, the study also tested a bare steel bar under similar loading conditions.

(a)

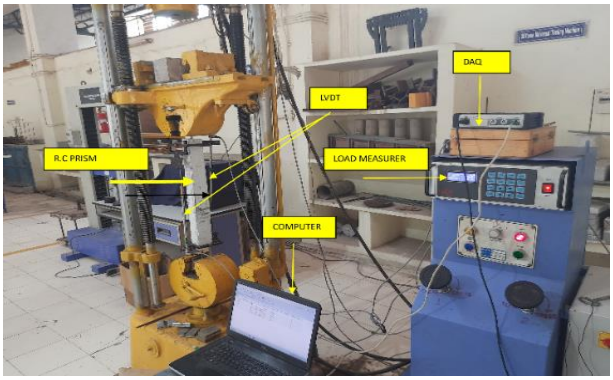

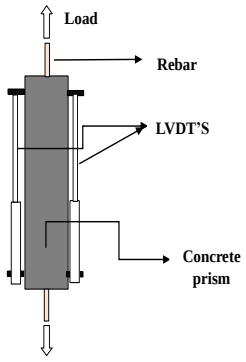

(b) (c)

Fig. 1. (a) cube, cylinder and prism testing (b) Uni-axial tension set up (c) Reinforced concrete prism with steel bar under uni-axial tension

4. Results and Discussion

4.1 Workability

Figures 2(a) and 2(b) illustrated the workability of mixtures in terms of slump values and reduction in slump in percentages. From Figs. 2(a) and (b), in all mix combinations, Slump values increased when fly ash was substituted with GGBFS from 0% to 100%. This indicates increasing workability. Earlier investigations also revealed that as the increase of GGBFS and NaOH concentration, the workability of AAC decreased [3,9,12]. This may due to the GGFBS particles have irregularly shaped and edged surfaces, while fly ash particles typically have round and smooth silt-sized particles. Hence, these small glass balls improve the flow and efficiency of fresh concrete as fly ash content increased. The highest decrement rate in mix-C was observed compared to mix-B and mix-A composites. From fig. 2(b), when the GGBFS percentage was increased from 0% to 100%, slump values decreased by 54.17% in mix A, 60.17% and 63.54% in mix B, C respectively.

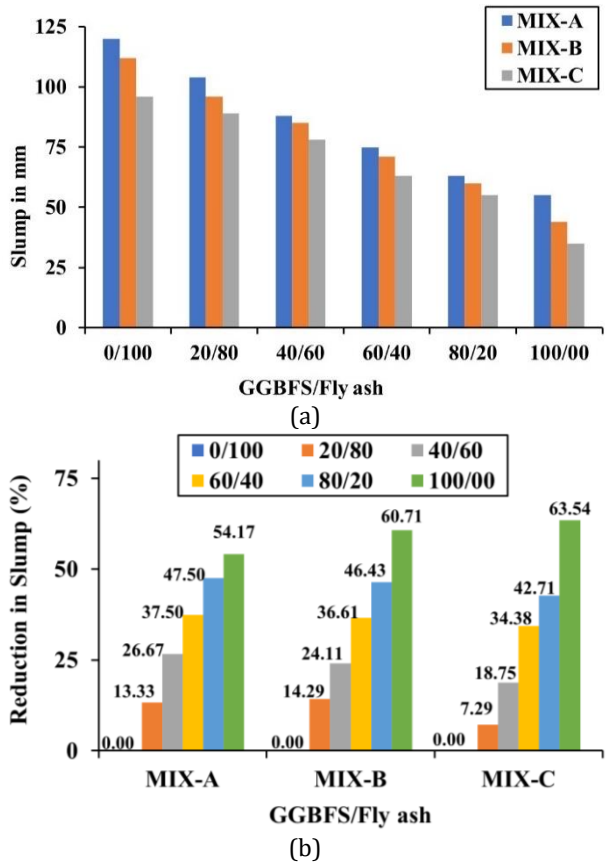

Fig. 2. (a) Workability of mixtures in terms of Slump values**,** 2(b) Reduction in slump in percentages with 100% fly ash (0/100 – GGBFS/Fly ash combination)

4.2.1 Compressive Strength

In Figs. 3(a), and (b) the 7-day and 28-day compressive strength results of all mixes are shown. The compressive strength values increased when the GGBFS content was increased from 0% to 100% in all mixes. In this study, maximum compressive strengths were achieved after 28 days curing in mix-A, mix-B, and mix-C at 100% GGBFS and 0% fly ash content, which are 27.03 MPa, 49.51 MPa, and 65.81 MPa in mix-A, B, and C respectively. Previous research has also indicated that GGFBS increases compressive strength, which may be attributed to the high calcium levels present in GGBFS [3,9-12]. But the obtained compressive strengths decreased as the fly ash content increased. This may due to the inclusion of fly ash reduces the Si/Al ratio in the mixture, indicating that determining the relative quantities of AlO^4 and SiO_4 generated in the geopolymer gel and determining the quantity of Si contained in the combination results in a low silicon/aluminum ratio that is associated with mixing with a high fly ash content. The compressive strength generally decreases as the Si/Al ratio decreases. The decrease in compressive strengths may due to the lower NaOH concentrations and provided curing conditions (i.e., ambient curing) in this study. The NaOH solution molarity plays the prominent role in dissolution of compounds present in source materials such as alumina and silica [5,6]. To obtain better geopolymerization, heat or high temperature curings are required when high fly ash levels are present in the mixes. But in this study all samples were cured at room temperature

only. The method of curing is also playing an important role in the geopolymerization process [3,5].

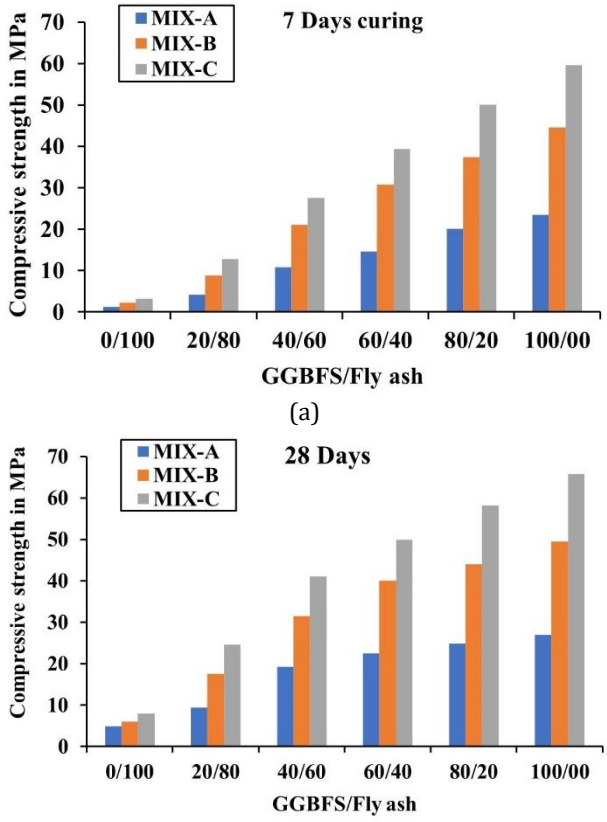

Fig. 3. Compressive strength values at various GGBFS and Fly ash proportions in mixes at: (a) 7 Days curing, (b) 28 Days curing

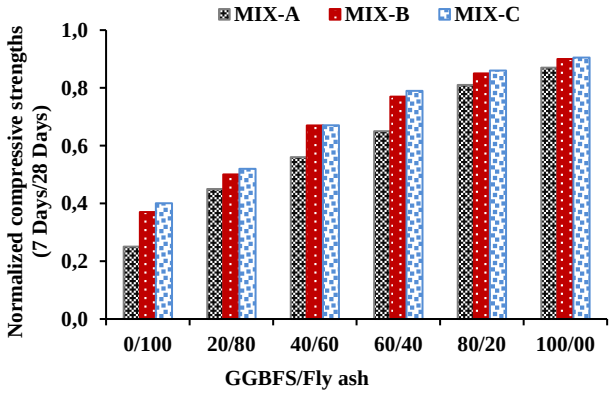

Fig. 4. Normalized compressive strengths (7 Days compressive strengths w.r.t 28 Days compressive strengths)

4.2.2 Early and Later Gain Strengths

The 7-day compressive strengths of all mixes are comparable to 28-day compressive strengths as depicted in Fig.4. When 100% GGBFS was used as a binder (reference mixes), most mixes gained 80%–90% of their total strength at an early age (at 7 days). Among all the mixes, the initial strength reduction percentage is the lowest in mix-C. Compared to mix-B and mix-C, the initial gain strength reduction percentage in mix-A was observed to be higher. Up to 2/3 of the initial strength was observed when GGBFS content of 60% was used in B and C mixtures, but not in the case of mix-A. This is because the reactivity of the alkaline solution with GGBFS content is higher at an early age than the reactivity of the alkaline solution with fly content, and huge amount of fly ash content slows down the hydration process, whereas GGBFS enhances the hydration process and reactivity.

4.2.3 Split Tensile and Flexural Strength

In Fig. 5, split tensile strength results for all mixes are shown. In all the mixes, as GGBFS increased, split tensile strengths increased. Split tensile strengths increased greatly as GGBFS in all mixes increased from 0% to 100% and the increment rate was very high at specimens having 60%, 80%, and 100% of GGBFS. However, these split tensile strengths decreased as fly ash in all mixes increased from 0% to 100% and the decrement rate was very high at 60%, 80%, and 100% fly ah containing specimens.

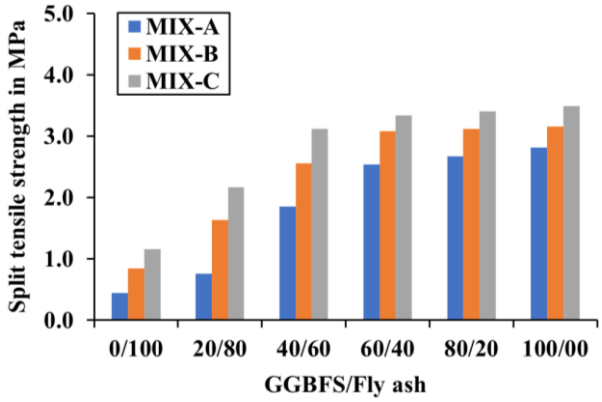

Fig. 5. Split Tensile strength values

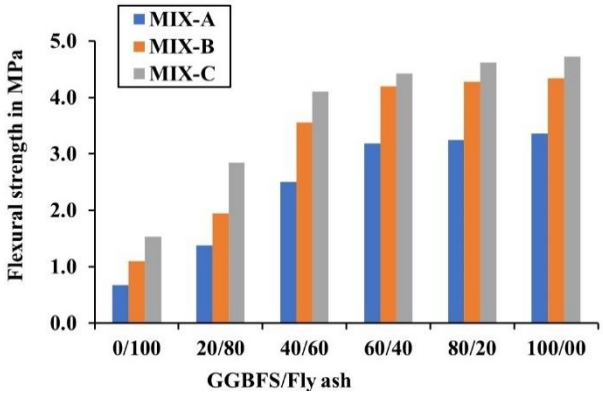

Fig. 6. Flexural strength values

In Fig. 6, the flexural strength results of all mixes are shown. As GGBFS content in all mixes increased from 0% to 100%, the flexural strength values increased. Diaz Loya et al. [41] also found that flexural strength values are higher for GGBFS content. But with the addition of 0%-40% GGBFS, flexural strength values decreased drastically, and the decrement rate was higher. Similar kind behaviour was reported by Sofi, M., et al. [42].

4.3 Tensile Behavior (Load-Member Strain Response)

To know the tensile behavior of specimens, first record the load displacement response. From this, the load-member strain response was obtained. The yield load and the first crack load were recorded and tabulated. The measured values first crack load, yield load and crack spacing are presented in Table 3. Similarly, average crack spacings, obtained from the present experimental study and various codes and previous studies, are given in Table 3. The first crack loads are increased as the GGBFS increased. From Table 3, in the mixes A, B and C yield loads in steel are slightly closer at 80% and 60% of GGBFS. This implies that fly ash and GGBFS combination increases the member's yield load carrying ability of steel bar when the member is in crack stabilization stage and after the first crack formation in the member.

Table 3. First Crack Loads, Yield loads and Crack Spacing details

Specimen designation (Mix-GGBFS/Fly Ash)	First crack load (kN)	Yield load in steel (kN)	Average crack spacing (mm)				
			Marti et al. [23] (OPC)	CEB - FIB Model [32] (OPC))	G. Kaklaus kas et al. [34] (OPC)	Experi mental (FSAAC)	No.of transv erse cracks
A-00/100	5.70	41.50	112.11	83.33	90.51	85.44	5
A-20/80	4.74	42.60	112.11	83.33	90.51	81.07	6
A-40/60	6.10	43.11	112.11	83.33	90.51	78.21	7
A-60/40	8.76	45.50	112.11	83.33	90.51	74.61	7
A-80/20	8.85	46.50	112.11	83.33	90.51	74.07	7
A-100/00	9.80	47.00	112.11	83.33	90.51	72.25	6
B-00/100	5.26	40.50	112.11	83.33	90.51	83.10	6
B-20/80	6.11	43.86	112.11	83.33	90.51	80.76	6
B-40/60	9.40	44.50	112.11	83.33	90.51	78.35	7
B-60/40	12.30	45.96	112.11	83.33	90.51	75.99	7
B-80/20	13.20	45.50	112.11	83.33	90.51	75.21	7
B-100/00	13.40	48.00	112.11	83.33	90.51	73.32	7
C-00/100	5.56	40.70	112.11	83.33	90.51	83.43	7
C-20/80	8.30	43.98	112.11	83.33	90.51	80.67	6
C-40/60	10.50	45.00	112.11	83.33	90.51	77.50	6
C-60/40	12.50	46.50	112.11	83.33	90.51	72.40	6
C-80/20	13.20	46.65	112.11	83.33	90.51	71.51	7
C-100/00	15.13	49.13	112.11	83.33	90.51	70.12	7

Figs. 7 (a), (b), and (c) illustrate the deformation response of the axis load member and a bare steel bar of mix-A, B, and C. The behaviour of the members is in starting linear as well as elastic until cracks appear in the concrete. After member develops cracks, the concrete contribution (average stress) decreased with increasing strain as more cracks form till cracking process stabilizes. Tension stiffening effect is slowly decreases after the crack is stabilized. Once the crack has stabilized, stiffness of members gradually decreased. The behaviour between cracks has the greatest influence on the tension stiffening of

conventional concrete [19]. After cracking, it can be observed that mixes having 100%-0% and 80%-20% GGBFS-fly ash exhibit more tension stiffening effect behavior than remaining mixtures. Similarly, all mixes also exhibited some desirable tension stiffening behavior when up to 60% of GGBFS was replaced. But when more than 60% of GGBFS was replaced, this tension-carrying capacity between the cracks was severely reduced. The reason for this is that as the fly ash increases, bonding between aggregates and the binder in the mixture decreases due to the better geopolymerization not achieved in the presence of small NaOH concentration and room temperature. Due to this, the bonding between concrete and steel can also decrease. Previous studies indicated that tension carrying capacity between cracks of concrete based on bond that occurred among concrete and steel; in relative to crack spacing, it established as per member cracks [29-31]. Tensile load carrying capacities at first crack load at different fly ash to GGBFS ratios, i.e., 0/100, 20/80, 40/60, 60/40, 80/20, and 100/0, while in Mix-A were 5.70 kN, 4.74 kN, 6.10 kN, 8.76 kN, 8.85 kN, and 9.80 kN, while in Mix-B were 5.26 kN, 6.11 kN, 9.40 kN, 12.30 kN, 13.20 kN, and 13.40 kN, and in Mix-C 5.56 kN, 8.30 kN, 10.50 kN, 12.50 kN, 13.20 kN, and 15.10 kN were observed, respectively. Similar results were observed in this study when compared with the studies of Albitar [32] and Ganesan et al. [45, 46]. In the Albitar [32] study, the first crack load was observed at 11.56 kN in fly ash-based GPC with a compressive strength of 35 MPa. Ganesan et al. [45] observed at 10 kN in plain fly ash-based GPC (FGPC) of M40-grade concrete. Ganesan et al. [46] study observed first crack load at 12.7 kN in plain fly ash and GGBFS-based GPC containing M40-grade concrete. In the present study, specimens that achieved 40 MPa compressive strength had a first crack load of 12.30 kN, 13.20 kN, and 13.40 kN in 60/40, 80/20, and 100/0 fly ash and GGBFS proportions of Mix-B mixes, respectively, and 12.50 kN in 60/40 fly ash and GGBFS proportions of Mix-C mixes. From this, it can be understood that fly ash and GGBFS combinations give better results than 100% fly ash specimens cured at room temperature. Similar behavior was observed in yield load as well.

In all mixes, whenever the GGBFS was rose to 80%, the load transfer of concrete among cracks was slightly similar compared to reference mixes (mixes having 100% GGBFS). When 0% GGBFS was used, all the mixes showed very low tensile strength, this may be due to the use of low concentrations of alkaline activated solution in the mixes and the lack of heat curing. Indeed, heat curing of concrete activated with fly-ash-based alkalis is essential for good polymerization [6]. But in our study, all the samples have been cured by ambient curing. As a result of the low concentration of the alkaline solution and the absence of heat curing, better hydration is not achieved at higher levels of fly ash contents. Tension stiffening effect was not effectively visible in A-mix compared to other two B and C mixes, since mix-A having low grade of strength of mixes. The tension stiffening capacity is more visible in members with a lower reinforcement ratio and higher concrete strength [43]. Mixes A, B, and C having 100%-0% and 20%-80% GGBFS-fly ash combinations showed slightly better tension stiffening effect compared to other mixtures.

Figures 8 (a), (b), and (c) demonstration the tensile stress in concrete over member strain of all specimens. It is evident that among all mixes, the specimens with high GGBFS gave better tensile stress values compared to those with lower GGBFS. In the mixes A, B and C, specimens having 100% GGBFS showed highest tensile stress values. Similarly, specimens with 80% GGBFS also gave better values; this is due to better bonding between concrete and steel. Bond effects were primarily responsible for the tension stiffening effect in cracked R.C. members [29-31].

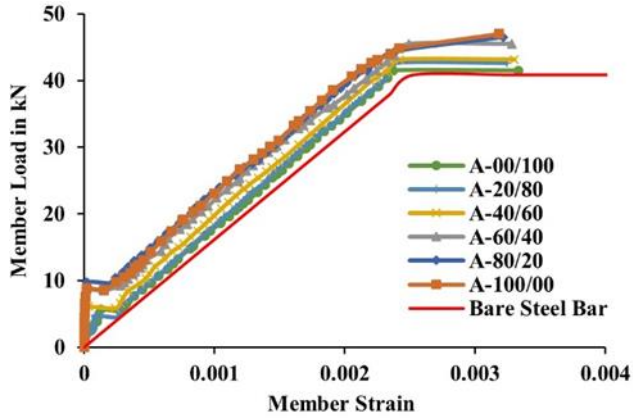

(a)

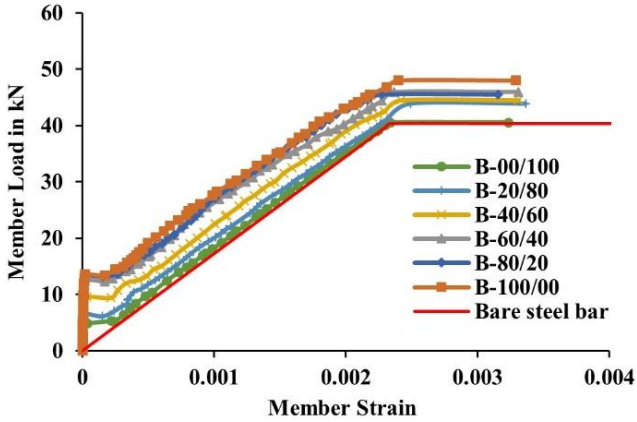

(b)

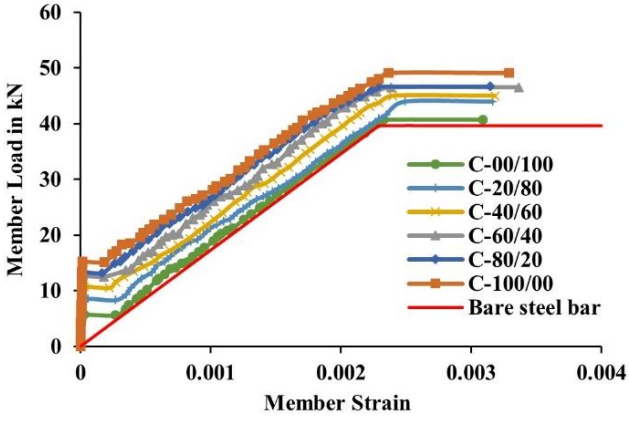

(c)

Fig. 7. Member Load vs Member Strain at various GGBFS and Fly ash ratios (a) Mix-A, (b) Mix-B, and (c) Mix-C

The maximum tensile stress of concrete in specimens was drastically reduced as the fly ash increased from the 0% to 100%. The maximum tensile stress of concrete at different fly ash to GGBFS ratios, i.e., 0/100, 20/80, 40/60, 60/40, 80/20, and 100/0, while in Mix-A were 0.93 MPa, 1.63 MPa, 2.39 MPa, 2.40 MPa, 2.6 MPa, and 2.41 MPa, while in Mix-B were 1.19 MPa, 1.80 MPa, 2.56 MPa, 3.46 MPa, 3.71 MPa, and 3.76 MPa, and in Mix-C 1.48 MPa, 2.14 MPa, 2.93 MPa, 3.52 MPa, 3.74 MPa, and 4.27 MPa were observed, respectively. Similar results were observed in this study when compared with the studies of Albitar [32] and Ganesan et al. [45, 46]. In the Albitar [32] study, the maximum tensile stress in concrete of 2.83 MPa was observed in fly ash-based GPC with a compressive strength of 35 MPa. Ganesan et al. [45] observed 2.5–3 MPa maximum tensile stress in plain FGPC of M40-grade concrete. Another Ganesan et al. [46] study observed 3–3.5 MPa maximum tensile stress in plain fly ash and GGBFS-based GPC containing M40 grade concrete. In the present study, specimens that achieved 40 MPa compressive strength had the maximum tensile stresses in concrete: 3.46 MPa, 3.71 MPa, and 3.76 MPa were observed in 60/40, 80/20, and 100/0 fly ash and GGBFS proportions in Mix-B mixes, respectively, and 3.52 MPa in 60/40 fly ash and GGBFS proportions in Mix-C mixes.

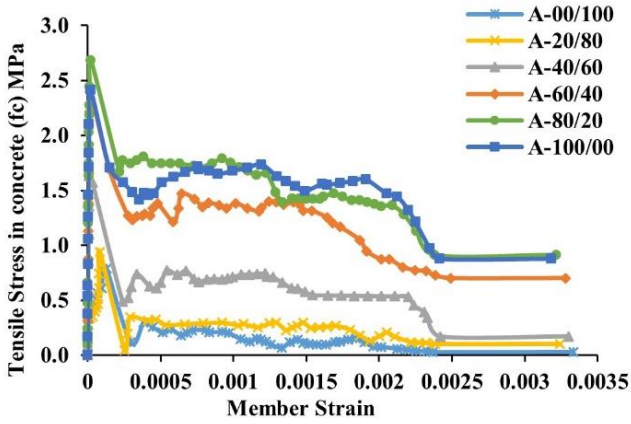

(a)

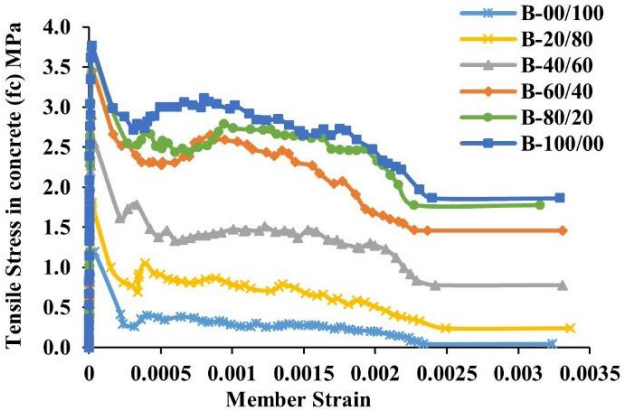

(b)

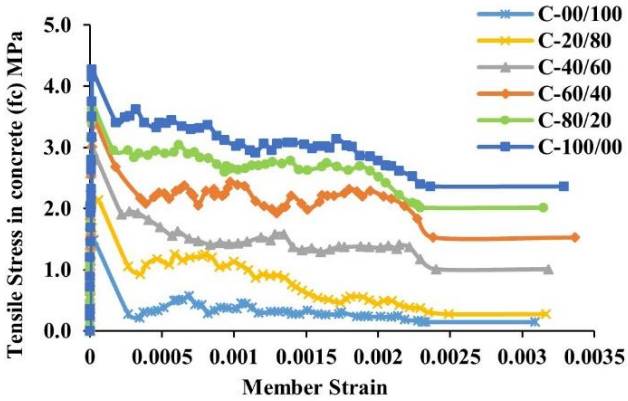

(c)

Fig. 8. Tensile stress in concrete vs Member strain at different GGBFS/Fly ash proportions (a) Mix-A, (b) Mix-B, and (c) Mix-C

4.4 Bond Factor or Tension Stiffening Bond Factor

In this investigation, bond factor (BF) is calculated by taking the ratio of average load carried by the cracked concrete to load carried by concrete at first crack. It is represented by "β" and its value generally varied between 0 to 1. In some cases, it may greater than 1. Better bond factor reveals that the better the member stiffness during the cracking of the member.

The bond factors of all mixes over member strain represented in Figures 9 (a), (b), and (c). In this context, if the bond factor is higher, which indicates that member stiffness is also higher, when compared to the remaining proportions in all the mixes, those mixes with 100% and 80% GGBFS content exhibited better bond factors. This indicates that the as the inclusion of fly ash in mixes, brittleness of member is decreased and enhance slightly the tension stiffening properties some extent. This is due to better bonding between concrete and steel. Since bond effects were primarily responsible for the tension stiffening effect in cracked R.C. members [29-31]. The bond factors dropped as fly ash content increases beyond 20%. This is due higher levels fly ash contents required better curing conditions and high molarity NaOH solutions. But in this investigation ambient curing and low molarity NaOH solutions are adopted.

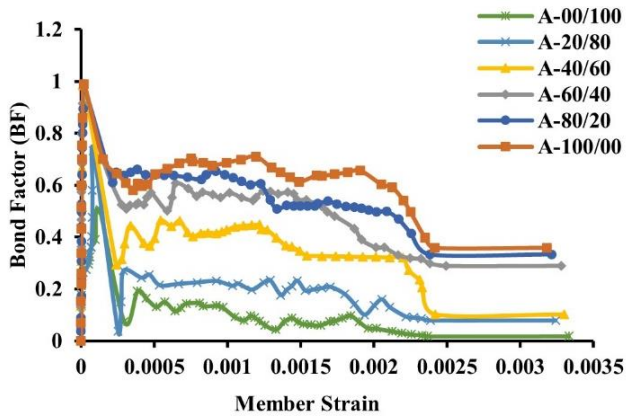

(a)

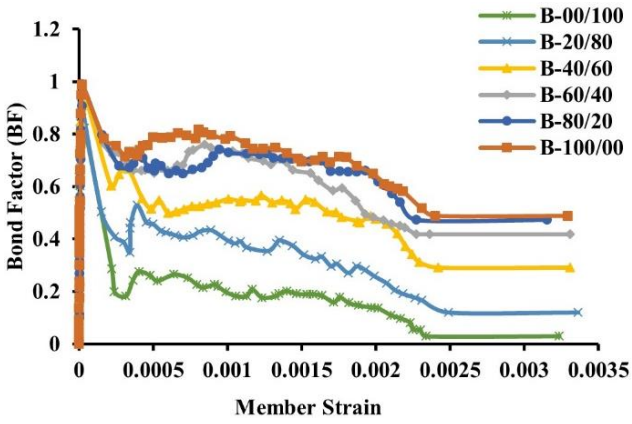

(b)

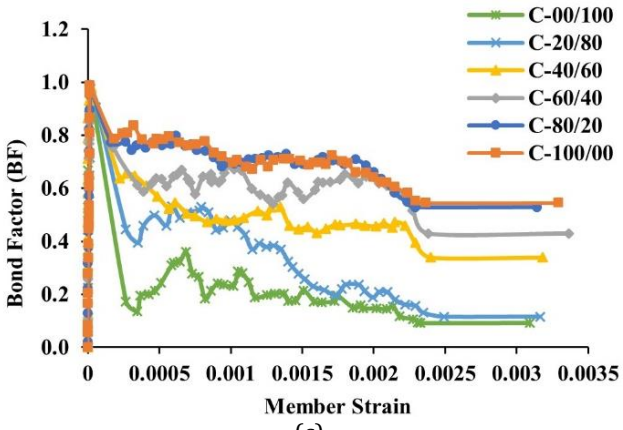

(c)

Fig. 9. Bond factor vs Member Strain at various GGBFS and Fly ash proportions (a) Mix-A, (b) Mix-B, and (c) Mix-C

The average bond factors improved as GGBFS content increased in all mixes. Among all the mixes, mix-C showed better average bond factor; these specimens indicated that there was better tension carrying capacity between the cracks after the first crack occurred. Similarly, all the mixes A, B, and C specimens having 60%–100% GGBFS had better bond factors and showed almost identical values at certain member strains. Mix-C specimens exhibited better average bond factors than mix-B and mix-A specimens, and mix-B specimens exhibited better average bond factors than mix-A. Overall, in all the mixes, the tension stiffening factor, or bond factor, varied from 0 to 1. Similar kinds of tension stiffening behaviour between the cracks (tension stiffening bond factor) were observed in this study when compared with the studies of Albitar [32] in fly ash-based GPC with a compressive strength of 35 MPa and plain FGPC of M40-grade concrete and plain fly ash and GGBFS-based GPC containing M40-grade concrete in Ganesan et al. [45, 46]. In Albitar [32] and Ganesan studies, the bond factors exist between 0 and 1. In Ganesan et al. [45, 46] studies, specimens having fly ash and the GGBFS combination exhibited better bond factors (tension stiffening behaviour between the cracks) compared to specimens having only fly ash. Similarly, in this study, specimens with fly ash and GGBFS combinations also exhibited better bond factors. Since better synergy existed between fly ash and GGBFS compared to fly ash as a sole binder.

4.5 Cracking Behavior

Cracking behavior is important in the limit state of serviceability of RC members. In this paper, an attempt is made to obtain a variation in the average crack spacing and the average maximum crack width as the load on the member increases and during the yield phase. Fig.10 illustrates the cracks formations and number of cracks of the tested prism. First crack formation was observed central region of the prism of most prisms, but two cracks also appeared at the same time in some members. The cracks that developed on all sides of the member were not uniform. When there is increasing in load, an increase in first crack width was observed.

Fig. 10. Crack patterns of the specimen

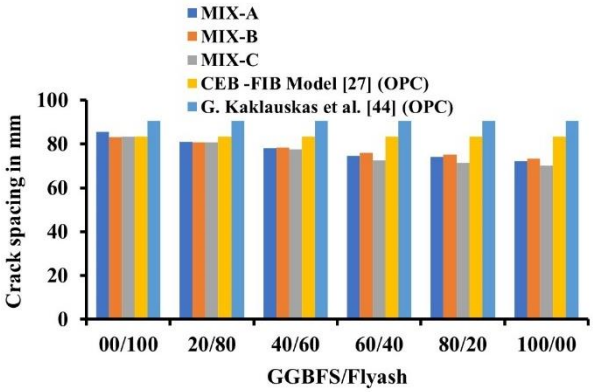

Fig. 11. Crack spacing comparison

Among all the mixes, minimum crack widths and reduced crack spacings were obtained at 100%, 80% and 60% GGBFS percentages. When GGBFS replacement exceeds 60%, both crack spacings as well as crack widths are increased. Fig.11 showed the average crack spacing in all the mixes, and these were compared with the CEB-FIB model code [27], as well as with proposed crack equations from G. Kaklauskas et al. [44]. The obtained values underestimated the CEB-FIB model code [27] and G. Kaklauskas et al. [44] equation some extent. But the variation observed between present experimental code and existed CEB-FIB model code [27] and G. Kaklauskas et al. [44] equation is below 10%. Ganesan et al. [45, 47] also reported that crack spacing for plain GPC consistent with CEB model code. Among all mixes, mixes containing 60% to 100% GGBFS had small crack spacing. This indicates that these mixes give better results from a serviceability point of view. Reduced crack spacing is frequently advantageous in terms of serviceability and plastic deformity aspect [47]. Closer results (crack spacings) were obtained in this study when compared with the studies of Ganesan et al. [45, 46], plain FGPC of M40-grade concrete, plain fly ash, and GGBFS-based GPC containing M40-grade concrete.

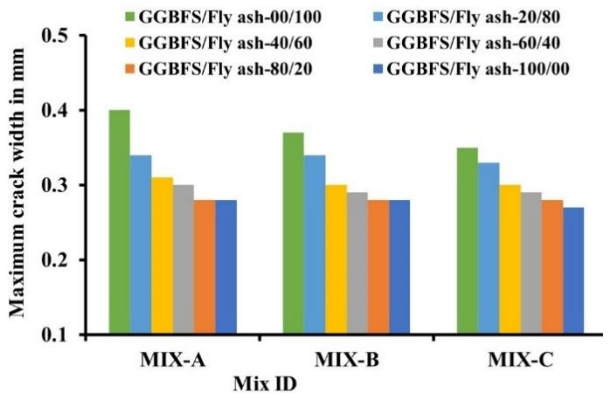

Fig. 12. Maximum crack width comparison

Ganesan et al. [45] observed 78.5 mm maximum average crack spacing in plain FGPC of M40-grade concrete. Another Ganesan et al. [46] study observed 73 mm maximum average crack spacing in plain fly ash and GGBFS-based GPC containing M40 grade concrete. In the present study, specimens that achieved 40 MPa compressive strength had the maximum average crack spacings in concrete: 83.1 mm, 80.76 mm, and 78.35 mm were obtained in 60/40, 80/20, and 100/0 fly ash and GGBFS proportions in Mix-B mixes, respectively, and 77.5 mm in 60/40 fly ash and GGBFS proportions in Mix-C mixes.

Fig.12 showed the maximum crack widths of all tested specimens. These crack width values were minimums in mixes having 100%, 80%%, and 60% GGBFS compared to the remaining mixes. Reduced spacings and narrow crack widths are obtained, when the members have 60%-100% GGBFS compared to the remaining mixes. Replacing GGBFS with fly ash increases workability, reduces brittleness and thereby improves fresh, strength and cracking properties to some extent. And also, the better bonding between concrete and steel existed in these proportions. This implies that the synergy between fly ash and GGBFS binder is greater than the sole binder (fly ash or GGBFS-based). The obtained crack widths (mixes having 40%-100 % GGBFS) are within permissible limits specified by CEB-FIB model code [27] and Eurocode-2 [28]. The obtained maximum average crack widths are closer and more consistent with the results obtained in Ganesan et al. [45, 46] studies. But underestimated results were obtained by Albitar [32].

5. Conclusions

In this study, fresh, tension stiffening (strength), and cracking characteristics of AAC with different proportions of fly ash and GGBFS has been investigated. From this study, it was found that

- The workability of all mixes in terms of slump has decreased with an increase in GGBFS content in the total binder from 0% to 100%. But slump values decreased with increased GGBFS. When the GGBFS percentage was increased from 0% to 100%, slump values decreased by 54.17% in mix A, 60.17% in mix B, and 63.54% in mix C. An increase in GGBFS content from 0% to 100% increased the compressive, split tensile and flexural strength of the composites under ambient curing. Due to low concentration of alkaline solution and lack of heat curing, better hydration is not achieved in mixtures with high fly ash percentages, resulting in low compressive strength of those specimens. Maximum compressive strength 27.03 MPa in mix-a, 49.51 MPa in mix-B, and 65.81 MPa in mix-C were obtained when

100% GGBFS as used as binder. Maximum compressive strengths were achieved after 28 days curing in mix-A, mix-B, and mix-C at 100% GGBFS and 0% fly ash content, which are 27.03 MPa, 49.51 MPa, and 65.81 MPa in mix-A, B, and C respectively.

- From the load-member strain response, in most of the mixes, tension stiffening effect improved as the GGBFS rose from 0% to 100%. Tension stiffening effect is slightly similar when mixes have 100%-0% and 80%-20% of GGBFS-fly ash proportions compared to all mixes after first crack. Among all the mixes, mix-C showed better average bond factor; these specimens indicated that there was better tension carrying capacity between the cracks after the first crack occurred. In the present study, specimens that achieved 40 MPa compressive strength had a first crack load of 12.30 kN, 13.20 kN, and 13.40 kN in 60/40, 80/20, and 100/0 fly ash and GGBFS proportions of Mix-B mixes, respectively, and 12.50 kN in 60/40 fly ash and GGBFS proportions of Mix-C mixes.
- Minimum crack widths and reduced crack spacings were obtained at 100%, 80% and 60% GGBFS percentages compared to the remaining mixes. This is due to the improved synergy between fly ash and GGBFS than that of the sole binder (fly ash). The calculated crack spacings are in good agreement with CEB-FIB model, and the variations in crack spacings are below 10%.
- Hence, through this study, it can be concluded when fly ash and slag-based alkali activated concretes were prepared with solutions containing low NaOH concentrations and cured at room temperature, there was a rise in the tension stiffening (strength) and cracking properties with higher percentages GGBFS.
- However, from this study, it is recommended that there is a need for a detailed parametric study to predict equations for cracking and tensile characteristics of plain and R.C. alkali-activated geopolymer concrete tension members to assess the structural behaviour of members under ambient curing conditions in any environmental condition. The bond between steel bar and concrete can also be considered an influencing parameter in the behaviour of FSAAC.

Acknowledgement

The authors acknowledge the support from NIT Warangal and the staff members of the material testing and Concrete Laboratory of the Department of Civil Engineering, NIT Warangal.

References

[1] Puertas F, Martínez-Ramírez S, Alonso S, Vázquez T. Alkali-activated fly ash/slag cements: Strength behaviour and hydration products. Cement and concrete research. 2000 Oct 1;30(10):1625-32. https://doi.org/10.1016/S0008-8846(00)00298-2

[2] Thunuguntla CS, Gunneswara Rao TD. Appraisal on strength characteristics of alkali-activated GGBFS with low concentrations of sodium hydroxide. Iranian journal of science and technology, transactions of civil engineering. 2018 Sep; 42:231-43. https://doi.org/10.1007/s40996-018-0113-4

[3] Mallikarjuna Rao G, Gunneswara Rao TD. Final setting time and compressive strength of fly ash and GGBS-based geopolymer paste and mortar. Arabian journal for science and engineering. 2015 Nov; 40:3067-74. https://doi.org/10.1007/s13369-015-1757-z

[4] Mallikarjuna Rao G, Gunneswara Rao TD, Siva Nagi Reddy M, Rama Seshu D. A study on the strength and performance of geopolymer concrete subjected to elevated temperatures. InRecent Advances in Structural Engineering, Volume 1: Select

Proceedings of SEC 2016 2019 (pp. 869-889). Springer Singapore. https://doi.org/10.1007/978-981-13-0362-3_70
[5] Karri SK, Ponnada MR, Veerni L. Development of eco-friendly GGBS and SF based alkali-activated mortar with quartz sand. Journal of Building Pathology and Rehabilitation. 2022 Dec;7(1):100. https://doi.org/10.1007/s41024-022-00235-5
[6] Phoo-ngernkham T, Maegawa A, Mishima N, Hatanaka S, Chindaprasirt P. Effects of sodium hydroxide and sodium silicate solutions on compressive and shear bond strengths of FA-GBFS geopolymer. Construction and Building Materials. 2015 Aug 30; 91:1-8. https://doi.org/10.1016/j.conbuildmat.2015.05.001
[7] Singh SP, Murmu M. Effects of curing temperature on strength of lime-activated slag cement. International Journal of Civil Engineering. 2017 Jun; 15:575-84. https://doi.org/10.1007/s40999-017-0166-y
[8] Bhowmick A, Ghosh S. Effect of synthesizing parameters on workability and compressive strength of fly ash based geopolymer mortar. International Journal of Civil & Structural Engineering. 2012;3(1):168-77.
[9] Lee NK, Lee HK. Setting and mechanical properties of alkali-activated fly ash/slag concrete manufactured at room temperature. Construction and Building Materials. 2013 Oct 1; 47:1201-9. https://doi.org/10.1016/j.conbuildmat.2013.05.107
[10] Hu Y, Tang Z, Li W, Li Y, Tam VW. Physical-mechanical properties of fly ash/GGBFS geopolymer composites with recycled aggregates. Construction and Building Materials. 2019 Nov 30; 226:139-51. https://doi.org/10.1016/j.conbuildmat.2019.07.211
[11] Nath P, Sarker PK. Effect of GGBFS on setting, workability and early strength properties of fly ash geopolymer concrete cured in ambient condition. Construction and Building materials. 2014 Sep 15; 66:163-71. https://doi.org/10.1016/j.conbuildmat.2014.05.080
[12] Fang G, Ho WK, Tu W, Zhang M. Workability and mechanical properties of alkali-activated fly ash-slag concrete cured at ambient temperature. Construction and Building Materials. 2018 May 30; 172:476-87. https://doi.org/10.1016/j.conbuildmat.2018.04.008
[13] Beeby AW, Scott RH. Cracking and deformation of axially reinforced members subjected to pure tension. Magazine of concrete research. 2005 Dec;57(10):611-21. https://doi.org/10.1680/macr.2005.57.10.611
[14] Chan HC, Cheung YK, Huang YP. Crack analysis of reinforced concrete tension members. Journal of Structural Engineering. 1992 Aug;118(8):2118-32. https://doi.org/10.1061/(ASCE)0733-9445(1992)118:8(2118)
[15] Gupta AK, Maestrini SR. Tension-stiffness model for reinforced concrete bars. Journal of Structural Engineering. 1990 Mar;116(3):769-90. https://doi.org/10.1061/(ASCE)0733-9445(1990)116:3(769)
[16] Lee GY, Kim W. Cracking and tension stiffening behaviour of high-strength concrete tension members subjected to axial load. Advances in Structural Engineering. 2009 Apr;12(2):127-37.
[17] Marti P, Alvarez M, Kaufmann W, Sigrist V. Tension chord model for structural concrete. Structural Engineering International. 1998 Nov 1;8(4):287-98. https://doi.org/10.2749/101686698780488875
[18] Yankelevsky DZ, Jabareen M, Abutbul AD. One-dimensional analysis of tension stiffening in reinforced concrete with discrete cracks. Engineering Structures. 2008 Jan 1;30(1):206-17. https://doi.org/10.1016/j.engstruct.2007.03.013
[19] Bischoff PH. Tension stiffening and cracking of steel fiber-reinforced concrete. Journal of materials in civil engineering. 2003 Apr;15(2):174-82. https://doi.org/10.1061/(ASCE)0899-1561(2003)15:2(174)
[20] Gribniak V, Mang HA, Kupliauskas R, Kaklauskas G. Stochastic tension-stiffening approach for the solution of serviceability problems in reinforced concrete:

Constitutive modeling. Computer-Aided Civil and Infrastructure Engineering. 2015 Sep;30(9):684-702. https://doi.org/10.1111/mice.12133
[21] Nayal R, Rasheed HA. Tension stiffening model for concrete beams reinforced with steel and FRP bars. Journal of materials in civil engineering. 2006 Dec;18(6):831-41. https://doi.org/10.1061/(ASCE)0899-1561(2006)18:6(831)
[22] Koeberl B, Willam K. Question of tension softening versus tension stiffening in plain and reinforced concrete. Journal of engineering mechanics. 2008 Sep;134(9):804-8. https://doi.org/10.1061/(ASCE)0733-9399(2008)134:9(804)
[23] Ian Gilbert R. Tension stiffening in lightly reinforced concrete slabs. Journal of Structural Engineering. 2007 Jun;133(6):899-903. https://doi.org/10.1061/(ASCE)0733-9445(2007)133:6(899)
[24] Kong KL, Beeby AW, Forth JP, Scott RH. Cracking and tension zone behaviour in RC flexural members. Proceedings of the Institution of Civil Engineers-Structures and Buildings. 2007 Jun;160(3):165-72. https://doi.org/10.1680/stbu.2007.160.3.165
[25] Muhamad R, Ali MM, Oehlers DJ, Griffith M. The tension stiffening mechanism in reinforced concrete prisms. Advances in Structural Engineering. 2012 Dec;15(12):2053-69. https://doi.org/10.1260/1369-4332.15.12.2053
[26] Abdulrahman H, Muhamad R, Azim MF. Tension stiffening behaviour of ordinary Portland and geopolymer concrete: A review. InAIP Conference Proceedings 2020 Oct 20 (Vol. 2284, No. 1). AIP Publishing. https://doi.org/10.1063/5.0027322
[27] Code, CEB-FIP Model. "Comité euro-international du béton." Bulletin d'information 213 (1995): 46.
[28] Eurocode 2 EN1992: Design of Concrete Structures (1992).
[29] Fields K, Bischoff PH. Tension stiffening and cracking of high-strength reinforced concrete tension members. Structural Journal. 2004 Jul 1;101(4):447-56. https://doi.org/10.14359/13330
[30] Bischoff PH. Effects of shrinkage on tension stiffening and cracking in reinforced concrete. Canadian Journal of Civil Engineering. 2001 Jun 1;28(3):363-74. https://doi.org/10.1139/l00-117
[31] Kaklauskas G, Gribniak V, Bacinskas D, Vainiunas P. Shrinkage influence on tension stiffening in concrete members. Engineering structures. 2009 Jun 1;31(6):1305-12. https://doi.org/10.1016/j.engstruct.2008.10.007
[32] Albitar M, Ali MM, Visintin P. Evaluation of tension-stiffening, crack spacing and crack width of geopolymer concretes. Construction and Building Materials. 2018 Jan 30; 160:408-14. https://doi.org/10.1016/j.conbuildmat.2017.11.085
[33] IS: 12089-1987, Specification for Granulated Slag for The Manufacture of Portland Slag Cement.
[34] IS 3812 (Part 1) :2003, Indian Standard Pulverized Fuel Ash Specification Part 1 for use as Pozzolana in Cement, Cement Mortar and Concrete.
[35] IS 383, "Indian Standard Coarse and Fine Aggregate for Concrete," Bureau of Indian Standards, (2016)
[36] IS 9103: 1999, Indian Standard Concrete Admixtures - Specification.
[37] Thunuguntla CS, Gunneswara Rao TD. Mix design procedure for alkali-activated slag concrete using particle packing theory. Journal of Materials in Civil Engineering. 2018 Jun 1;30(6):04018113. https://doi.org/10.1061/(ASCE)MT.1943-5533.0002296
[38] IS:7320 - 1974, specification for concrete slump test apparatus.
[39] IS: 516 - 1959, Indian Standard methods of tests for strength of concrete.
[40] ASTM C-293-02, "Standard Test Method for Flexural Strength of concrete (using Simple Beam with Center-Point Loading)," International Standard Organization, (2002).
[41] Diaz-Loya EI, Allouche EN, Vaidya S. Mechanical properties of fly-ash-based geopolymer concrete. ACI materials journal. 2011 May 1;108(3):300. https://doi.org/10.14359/51682495

[42] Sofi M, Van Deventer JS, Mendis PA, Lukey GC. Engineering properties of inorganic polymer concretes (IPCs). Cement and concrete research. 2007 Feb 1;37(2):251-7. https://doi.org/10.1016/j.cemconres.2006.10.008

[43] Khalfallah S, Guerdouh D. Tension stiffening approach in concrete of tensioned members. International Journal of Advanced Structural Engineering. 2014 Mar; 6:1-6. https://doi.org/10.1007/s40091-014-0051-8

[44] Kaklauskas G, Ramanauskas R, Ng PL. Predicting crack spacing of reinforced concrete tension members using strain compliance approach with debonding. Journal of Civil Engineering and Management. 2019 May 2;25(5):422-30. https://doi.org/10.3846/jcem.2019.9871

[45] Ganesan N, Indira PV, Santhakumar A. Influence of steel fibres on tension stiffening and cracking of reinforced geopolymer concrete. Magazine of concrete research. 2014 Mar;66(6):268-76. https://doi.org/10.1680/macr.13.00273

[46] Ganesan N, Sahana R, Indira PV. Effect of hybrid fibers on tension stiffening of reinforced geopolymer concrete. Advances in concrete construction. 2017 Feb;5(1):075. https://doi.org/10.12989/acc.2017.5.1.75

[47] Zwicky D. Bond and ductility: a theoretical study on the impact of construction details-part 1: basic considerations. Advances in concrete construction. 2013 Mar;1(1):103. https://doi.org/10.12989/acc.2013.1.1.103